STOCHASTIC SEISMIC EMISSION FROM ACOUSTIC GLORIES AND THE QUIET SUN

A.-C. DONEA[1], C. LINDSEY[2] and D.C. BRAUN[2,*,†]
[1]*Astronomical Institute of the Romanian Academy, Cutitul de Argint 5, RO-75212, Bucharest, Romania (E-mail:adonea@roastro.astro.ro)*
[2]*Solar Physics Research Corporation, 4720 Calle Desecada Tucson, AZ 85718, U.S.A. (E-mail:lindsey@sprc.com; dbraun@solar.stanford.edu)*

(Received 21 September 1999; accepted 8 January 2000)

Abstract. Helioseismic images of multipolar active regions show enhanced seismic emission in 5-mHz oscillations in a halo surrounding the active region called the 'acoustic glory'. The acoustic glories contain elements that sustain an average seismic emission 50% greater than similar elements in the quiet Sun. The most intense seismic emitters tend to form strings in non-magnetic regions, sometimes marking the borders of weak magnetic regions and the separation between weak magnetic regions of opposite polarity. This study compares the temporal character of seismic emission from acoustic glories with that from the quiet Sun. The power distribution of quiet-Sun seismic emission far from solar activity is exponential, as for random Gaussian noise, and therefore not perceivably episodic. The distribution of seismic power emanating from the most intense elements that comprise the acoustic glories is exponential out to approximately 4 times the average power emitted by the quiet Sun. Above this threshold the latter distribution shows significant saturation, suggesting the operation of a hydromechanical non-linearity that sets limits on the acoustic power generated by the convection zone. This could give us considerable insight into the physical mechanism of seismic emission from the near subphotosphere.

1. Introduction

Techniques in local helioseismology now allow us to make high-quality seismic images of the surfaces and near interiors of active regions. The general concept of seismic imaging of local solar interior structure was advanced by Lindsey and Braun (1990), Braun *et al.* (1992), Lindsey *et al.* (1996), and Lindsey and Braun (1997) under the term 'helioseismic holography' as a crucial diagnostic basis of local helioseismology. The application of holographic imaging to helioseismic observations from SOHO-MDI has now given us a broad range of discoveries. These include 'acoustic moats' (Braun *et al.*, 1998; Lindsey and Braun, 1998a), 'acoustic glories' (Braun and Lindsey, 1999), subsurface acoustic condensations beneath sunspots (Lindsey and Braun, 1998b) and multipolar active regions (Braun and

*Visitor, Joint Institute for Laboratory Astrophysics, U. Colorado, Boulder, CO 80309-0440, U.S.A.
†Current mailing address: Colorado Research Associates, 3380 Mitchell Lane, Boulder, CO 80301, U.S.A.

Solar Physics **192:** 321–333, 2000.

Lindsey, 1999), and helioseismic images clearly showing the spatial extension of acoustic emission from a large solar flare (Donea, Braun, and Lindsey, 1999).

Holographic images of seismic emission in well-developed active regions in the 2.5−4.5 mHz spectrum invariably show a dense halo of seismic deficit extending 30 Mm or more outside of surface magnetic regions. Above 4.5 mHz, the seismic emission deficit persists in the magnetic region itself. However, for large, multipolar active-region complexes, the extended halo of seismic emission deficit that characterizes the acoustic moat is replaced by an acoustic glory, a halo that shows sharply *enhanced* seismic emission, largely from small, point-like elements that tend to form thin, beady strings. In fact, a measurable enhancement in seismic emission actually exists around single monopolar sunspots (Lindsey and Braun, 1999), approximately 2.5% above that of the seismic emission from the surrounding quiet Sun, but this is subtle and diffuse. It is only around large-multipolar active regions that the acoustic glory is prominent (Braun and Lindsey, 1999), showing seismic emission averaging roughly 15% in excess of the mean quiet Sun.

An example of an acoustic glory is shown in Figure 1. Figure 1(a) shows a seismic emission map of NOAA Active Region 8179 in the 4.5−5.5 mHz band, made from SOHO-MDI Doppler observations integrated over the 24 hr period beginning at 15 March 1998. Directly below it, Figure 1(b), is an MDI magnetogram. The seismic emission in the surface magnetic regions is significantly depressed, to ∼50% of the quiet-Sun emission. The acoustic glory appears as a bright halo surrounding the active region. It is largely comprised of small, discrete seismic emitters that tend to cluster in strings in non-magnetic regions. The individual small-scale emitters comprising the strings are at the acoustic diffraction limit of the 5 mHz acoustic images attainable from the medium-resolution MDI images, ∼3 Mm. A single such emitter may maintain a time-averaged seismic egression power well in excess of 1.5 times that of the mean quiet Sun. Some of these emitters are marked with numbered points in Figures 1(c) and 1(d) to identify their locations with respect to magnetic regions. These locations as seen in the magnetogram (Figure 1(d)) show that the individual emitters substantially appear only in non-magnetic regions, but nevertheless with a remarkable tendency to border weak magnetic regions. Along the north-east boundary of NOAA AR 8179 (markers 3, 4, 7−13), the acoustic glory marks a thin gap separating weak magnetic regions of opposite polarity.

As we have mentioned (Braun and Lindsey, 1999), isolated monopolar sunspots show only a relatively weak, diffuse acoustic glory that is not at all conspicuous. The single sunspot to the north-east (upper left) of NOAA AR 8179 is typical.

Acoustic glories, then, could give us great insight into the physical mechanism of seismic emission from the quiet Sun. The purpose of this study is to examine the *temporal* character of the seismic emission from the individual small-scale emitters that comprise the acoustic glories. We are particularly interested in whether the seismic emission from these features is significantly episodic. In the interests of control work, we have applied the same diagnostic to the quiet Sun.

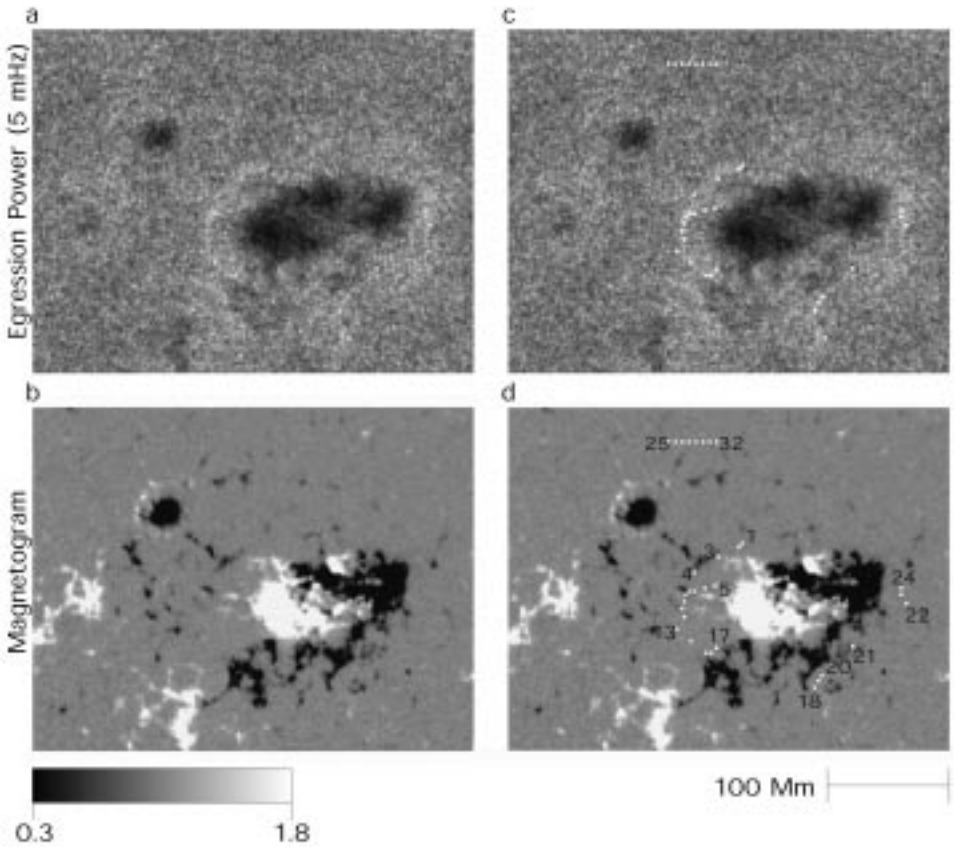

Figure 1. Seismic egression-power map (a) of NOAA AR 8179 in a 1 mHz band centered at 5 mHz, integrated over the 24-hr interval beginning at 15 March 1998. (b) shows the SOHO-MDI magnetogram obtained at 15 March 1998. Frames (c) and (d) show reference points superimposed onto the respective egression-power map and SOHO magnetogram to indicate the locations of small-scale elements of enhanced seismic emission which comprise the 5-mHz solar acoustic glories. In Frame (d), the reference points are numbered counter-clockwise proceeding around the active region to identify samples of acoustic power to be plotted in Figure 2. The row of eight points labeled 25−32 near the top of the frame show locations chosen for control measurements in the quiet Sun. The greyscale at lower left applies to the egression power maps. The greyscale of the magnetograms saturates at ±200 G.

2. Seismic Holography

The basic concept of seismic imaging is described by Lindsey and Braun (1997). Seismic disturbances measured at the solar surface are applied to an acoustic model of the quiet Sun and propagated in time reverse into the model interior to render wave-mechanical images of the acoustic field beneath the photosphere. This regressed acoustic field is called the 'coherent seismic egression'. In the case of solar acoustics, waves emitted downward from the surface are predominantly refracted

back to the surface. Holographic imaging thus makes it possible to render seismic sources at the solar surface using waves that have traveled far beneath the photosphere to resurface in the quiet Sun tens of Mm from the source.

For waves less than 2.5−4.5 mHz frequency, the near subphotosphere is an efficient specular reflector, and these waves generally skip to the surface many times before their coherence is destroyed, probably by Doppler perturbations encountered in the supergranulation within a few Mm of the photosphere. Accordingly, holographic reconstruction can be and is accomplished for disturbances that have skipped to the surface several times (Braun *et al.*, 1998).

The photosphere effectively absorbs seismic disturbances above ∼4.5 mHz in frequency. These frequencies can therefore be imaged only the distance of a single horizontal skip. However, these waves offer the advantage of a finer diffraction limit and superior depth discrimination (Lindsey and Braun, 1998b; Braun and Lindsey, 1999). Moreover, distinctive signatures that appear in egression power images in this part of the spectrum can be interpreted unambiguously as seismic sources where they appear, not a specular reflection of acoustic energy that has originated somewhere else.

In this study, we have undertaken to use seismic holography to examine the temporal character of the individual small-scale seismic sources that comprise the acoustic glories. In particular, we show the temporal profiles of 4.5−5.5 mHz seismic emission emanating from the points shown in Figure 1. Control measurements from the quiet Sun are taken from reference points 25−32 in Figure 1(d), which appear in a horizontal row near the northern boundary of the frame.

The computations reported here were made from data taken with the SOI-MDI instrument spanning the 24-hr period beginning on 15 March 1998 while a large active-region (NOAA AR 8179) was close to the central meridian. The SOI-MDI instrument and its data products are described in detail by Scherrer *et al.* (1995). The data we analyzed consist of full-disk 1024 × 1024 pixel (medium-resolution) Dopplergrams obtained once per minute nearly continuously during one of the high-telemetry rate 'Dynamics' campaigns.

3. Temporal Character of Seismic Emission

The temporally discriminating seismic holography applied in this study is essentially identical to that reported by Donea, Braun, and Lindsey (1999) to the large solar flare of 9 July 1996, whose seismic signature was discovered by Kosovichev and Zharkova (1998). In standard seismic holography, the observed surface acoustic field, $\psi(\mathbf{r}', t')$, is propagated in time reverse from its horizontal location and time $(\mathbf{r}', t')$ to a location and time $(\mathbf{r}, z, t)$ at depth z, by convolution with a Green's function, G_+, to render a regressed acoustic field which we call the egression:

$$H_+(z, \mathbf{r}, t) = \int \mathrm{d}t' \int\limits_{a<|\mathbf{r}-\mathbf{r}'|<b} \mathrm{d}^2\mathbf{r}'\, G_+(z, \mathbf{r}, t, \mathbf{r}', t')\, \psi(\mathbf{r}', t') \,. \tag{1}$$

In our case, the computation is made over an annular acoustic pupil of inner radius $a = 15.3$ Mm and outer radius $b = 44.5$ Mm. The surface is assumed to be a perfect absorber, and so the Green's function is truncated after a single skip to the surface. The computation expressed by Equation (1), then, coherently regresses the acoustic field a single skip, from the observed surface disturbance to the surface point at which it is supposed to have originated. Since all of the egressions computed in this study are computed at the surface, $z = 0$, we omit this argument in the following discussion.

For the purpose of considerably improved numerical efficiency, the computation was made in the 'spectral perspective' described by Lindsey and Braun (1997), which directly renders the temporal Fourier transform, $\hat{H}_+(\mathbf{r}, \nu)$, of $H_+(\mathbf{r}, t)$, such that

$$H_+(\mathbf{r}, t) = \int\limits_{-\infty}^{\infty} \mathrm{d}\nu\, e^{2\pi i \nu t}\, \hat{H}_+(\mathbf{r}, \nu) \,. \tag{2}$$

For our application, a complex variant of the egression expressed above is obtained by computing the above integral only over a selected positive frequency band, $\Delta\nu = 1$ mHz, that is centered at 5 mHz. The egression power in this band is simply the real modulus of the resulting complex amplitude:

$$P(\mathbf{r}, t) = |H_+(\mathbf{r}, t)|^2 \,. \tag{3}$$

The restriction to a limited frequency band is accomplished at a significant expense in temporal resolution: $\Delta t = 1/\Delta\nu = 1000$ s, in accordance with the Heisenberg principle.

As in Donea, Braun, and Lindsey (1999), the egression computations for this study were made with a Green's function, G_+, that takes full account of dispersion of the seismic spectrum by the near subphotosphere. The convenient extension of the dispersionless Green's function described in Lindsey and Braun (1997) to take account of dispersion is explained in Lindsey and Braun (2000). Dispersion can be critical when the analyst is concerned with the temporal profile of the egression.

4. Results

The individual egression-power time series of the points indicated by the markers 1–16 in Figure 1(d), computed as prescribed in the previous section, are shown in Figure 2. The complex egression amplitude (see Equation (2)) for each marker is averaged over a 2 pixel × 2 pixel (2.8 Mm × 2.8 Mm) square region centered on the

marker and its absolute value is squared as prescribed by Equation (3). These time-series are successively plotted in the Figure, the number identifying each location appearing at the left of its respective plot. Control points, taken from the quiet Sun, are represented by the markers indexed by 25–32.

For purposes of further control, we computed the *ingression* powers of the quiet-Sun markers. The acoustic ingression, $H_{-}(z, \mathbf{r}, t)$, is equivalent to the egression computation of the time-reversed acoustic disturbance (see Lindsey and Braun, 1997). It expresses disturbances that happen to be *converging* coherently *towards* the focus rather than emanating from it. Ingression powers for the control pixels are plotted in Figure 2 directly below the egression-power time series. These give us an expected random Gaussian noise.

The difference between the egression power plots representing the acoustic glory and those representing the quiet Sun are fairly conspicuous. The seismic power from emitters in the acoustic glory is generally sustained at a significantly greater level than from the quiet Sun. By comparison to the acoustic glories, the egression power time series representing acoustic emitters in the quiet Sun appear somewhat episodic. For random Gaussian noise, the distribution, $D(|H^2|)$ in egression power $|H|^2$ should be simply exponential:

$$D(|H^2|) \;=\; \exp\left(-|H|^2/H_0^2\right) , \tag{4}$$

with H_0 representing the root mean power, $\langle |H|^2 \rangle^{1/2}$, of the noise. If an egression power time series contains a component of acoustic emission that is substantially episodic, this should result in a significant departure of the egression-power distribution, D, from the nominal exponential profile. In particular, $D(|H|^2)$ would be significantly increased at the higher values of its argument, $|H|^2$, by the sporadic enhancement contributed by the episodic component.

Figure 2 actually illustrates how appearances can be misleading when Gaussian noise is plotted in comparison with anomalous emitters that themselves turn out to be non-Gaussian. It is the egression power of the acoustic glory, not the quiet Sun, that departs significantly from an exponential distribution. The distribution, D, of egression power from the points labeled 1–24 in Figure 1(d), those which identify the most conspicuous emitters in the acoustic glory surrounding NOAA AR 8179, is plotted in Figure 3(a). This profile is defensibly exponential out to approximately four times the average quiet-Sun egression, H^2_{quiet}, satisfying Equation (4), with $H_0^2 = 1.51\ H^2_{\text{quiet}}$. Above an egression power of $4H^2_{\text{quiet}}$, a significant saturation develops.

Distributions of egression power in the quiet Sun appear to show a slight variation, depending on location. In the quiet Sun, 50–70 Mm, outside of NOAA AR 8179, the egression power distribution sometimes shows a slight *enhancement* at 6–8 times the mean egression power of the quiet Sun, H^2_{quiet} in place of the saturation that characterizes the acoustic glory. This enhancement accounts for no more than a few percent of the total egression power and suggests contamination of the outlying neighborhood of the active region by occasional glory-like emission.

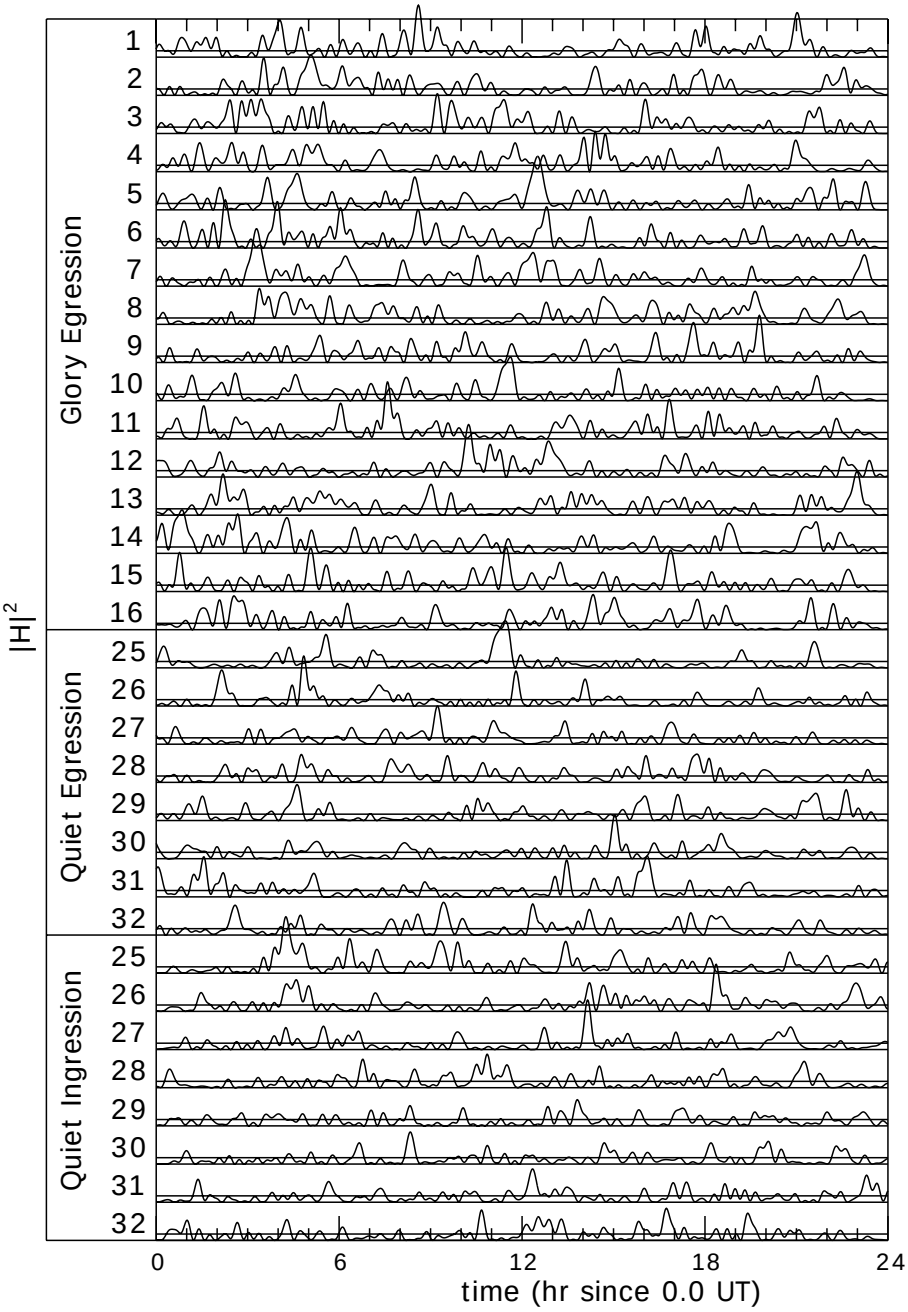

Figure 2. Time series of egression power in 1-mHz bands centered at 5 mHz. The 5-mHz egression amplitude was averaged over 4-pixel elements, each covering an area of $\sim$8.0 Mm^2, the 5-mHz seismic diffraction limit. The square of the absolute value of this complex amplitude is plotted for locations 1–16 in Figure 1(d). The number to the left of each plot identifies the location in Figure 1(d) from which the time-series was taken. Time-series numbered 25–32 sample the control reference points at the top of Figure 1(d). Both the ingression and egression powers of the control points are plotted. Horizontal lines above the base of each plot indicate the average egression power of the quiet Sun.

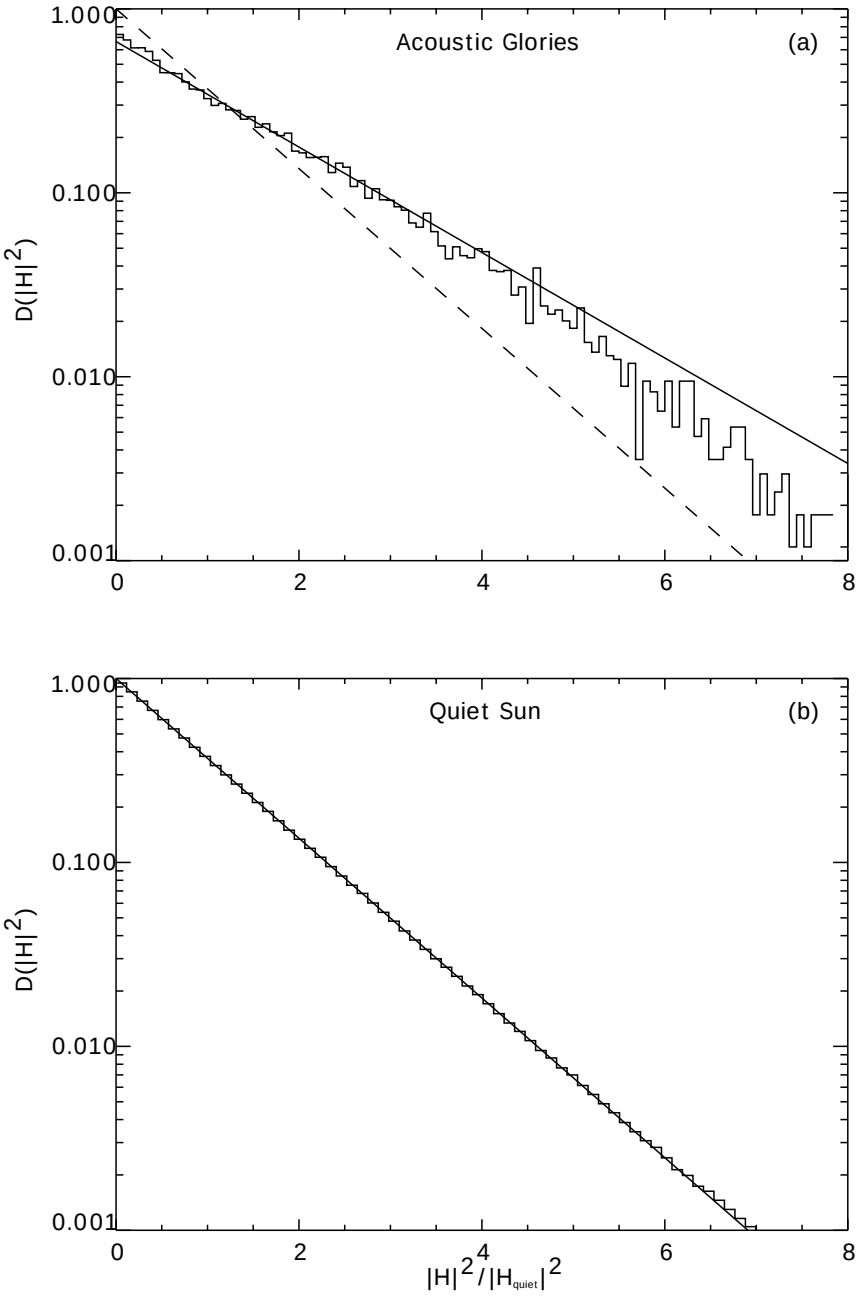

Figure 3. Distributions of 5-mHz egression power in (a) the acoustic glory (upper frame) and in (b) the quiet Sun (lower). Statistics for the acoustic glory are taken from the 4-pixel elements located at points 1–24 in Figure 1(d), the time-series for points 1–16 of which are plotted in Figure 2. Statistics for the quiet Sun are taken from a region some 24 000 Mm^2, in area centered 34° north-west of NOAA AR 8179. This area is approximately 3000 times the 5 mHz seismic diffraction limit. The egression powers (abscissa) are normalized to that of the mean quiet Sun. The solid line in Figure 3(a) renders the distribution $\exp(-|H|^2/H_0^2)$, with $H_0^2 = 1.51\ H_{\rm quiet}^2$. The dashed line in Figure 3(a) and the solid line in (b) render the same with $H_{\rm quiet}^2$.

Distributions of egression power from the quiet Sun far from magnetic regions (Figure 3(b)) show a profile that is accurately exponential out to at least $8H^2_{\text{quiet}}$. This is consistent with sustained, random Gaussian noise, which is what is generally exhibited by all ingression-power time series. Seismic emission from the quiet Sun far from solar activity is therefore not perceivably episodic on the 8 Mm^2 spatial scale discriminated by the MDI medium-resolution Dopplergrams. Instances of apparent episodic emission in the quiet-Sun time series plotted in Figure 2, then, are what can be expected as a result of statistical accident, and are not significant of a mechanism of seismic emission that is otherwise substantially episodic in nature.

5. Discussion and Conclusions

It should be borne in mind that a considerable portion of the disturbance that appears in an egression computation necessarily represents something other than what was intended. The intent is a coherent reconstruction of radiation that propagated downward from the focal point, **r**, of the computation (see Equation (1)), and refracted back upward to arrive at the pupil many Mm from the source. However, acoustic disturbances can generally propagate upwards as well as downwards, as far as we know. The egression computation must therefore also yield an *incoherent* representation of locally generated acoustic radiation from the subphotosphere just beneath the pupil that propagated upward directly into the pupil. While we cannot rule out the possibility, it is difficult to conceive of a scheme whereby these two components would be significantly unequal. We think that realistically approximately half of the egression power that appears at any particular focal point, **r**, in the quiet Sun can be regarded as incoherent noise superimposed onto a coherent representation of the disturbance actually generated in the neighborhood of that focal point.

Braun *et al.* (1992), Brown *et al.* (1992), Toner and LaBonte (1993), and Hindman and Brown (1998) noticed conspicuous halos surrounding plages and sunspots in plain acoustic power maps of 6-mHz oscillations, suggesting that these may be regions of enhanced seismic emission. This has transpired not to be generally the case. It is critical to keep the distinction between the enhanced seismic *emission* that characterizes acoustic glories and the localized enhancement of the *surface disturbance* that registers the arrival of an underlying wave. It is particularly the *surface disturbance*, not necessarily excess *seismic emission*, that generally gives rise to the acoustic power halos. Acoustic power halos surround all active regions, including isolated monopolar sunspots and plages. Intense acoustic glories surround only large, multipolar active regions (Braun and Lindsey, 1999). A fairly graphic example of this distinction is shown in Figure 4, which compares a 6-mHz acoustic power map of NOAA AR 8179 (Figure 4(a)) with the 5-mHz acoustic egression map of the same (Figure 4(b)). Acoustic power halos surround all substantial active regions in Figure 4(a), including the isolated, monopolar sunspot to

the north-east of NOAA AR 8179. However, the monopolar sunspot is conspicuously missing a noticeable acoustic glory. Acoustic power halos are seen in both photospheric Doppler oscillations and calcium K-line intensity oscillations at 5–6 mHz. However, Hindman and Brown (1998) have pointed out that these features do not substantially appear in visible continuum oscillations.

Based on theoretical work by Goldreich and Kumar (1988), Brown (1991) suggested that seismic emission from the near subphotosphere due to convective turbulence should be relatively localized at any particular moment. This was based on the understanding that the flux of dipole and quadrupole emission due to turbulence should be a strong function of the turbulent velocity, and the working assumption that the velocity distribution of the near convection zone is Gaussian. Let us suppose that the turbulence is distributed randomly over the quiet solar surface, and that the lifetime of a single convective granule is short, of order 10 min. The ergodic principle applied to these assumptions secures that seismic emission that is spatially localized is likewise episodic. If the seismic emission at any one time is predominantly concentrated into relatively localized regions, and those regions are randomly redistributed after a single convective lifetime, then turbulent emission from any arbitrary location must be concentrated into relatively localized *time* intervals.

Deubner *et al.* (1992) have pointed out the utility of phase correlation diagnostics between velocity and intensity to distinguish between local convective disturbances and ambient waves impinging from distant sources. Moretti and Jefferies (1999, private communication) have emphasized this concept, bearing in mind that convective disturbances may be signatures of local wave generation. Recent observational work by Goode *et al.* (1998) examines spectral signatures that are intended to discriminate locally generated waves from the ambient background. Based on the signatures their observations have rendered, they propose that wave generation by the near subphotosphere is quite localized and episodic and generally related to the collapse of intergranular lanes.

The distributions plotted in Figure 3 do not support the proposition that a substantial fraction of the 5 mHz acoustic flux generated by the quiet Sun is episodic, at least on the 8 Mm^2 spatial scale discriminated by the medium-resolution MDI Dopplergrams. If acoustic emission from the near subphotosphere is substantially episodic in nature, the quiet-Sun egression power distributions suggest that the distance and time scales that separate individual episodes must be substantially finer than 8 Mm^2. It should be kept in mind that spatial resolution matters. The high-resolution MDI observations should improve our resolution in area by nearly an order of magnitude. This may possibly allow us to separate episodes that the holographic images in this study cannot discriminate.

A more recent study (Rimmele, 1999, private communication) finds that the episodes, which they propose are related to wave emission, occur with significantly more intensity in the quiet Sun immediately outside of active regions than far from active regions. While it is much too early to secure a firm conclusion, this new find-

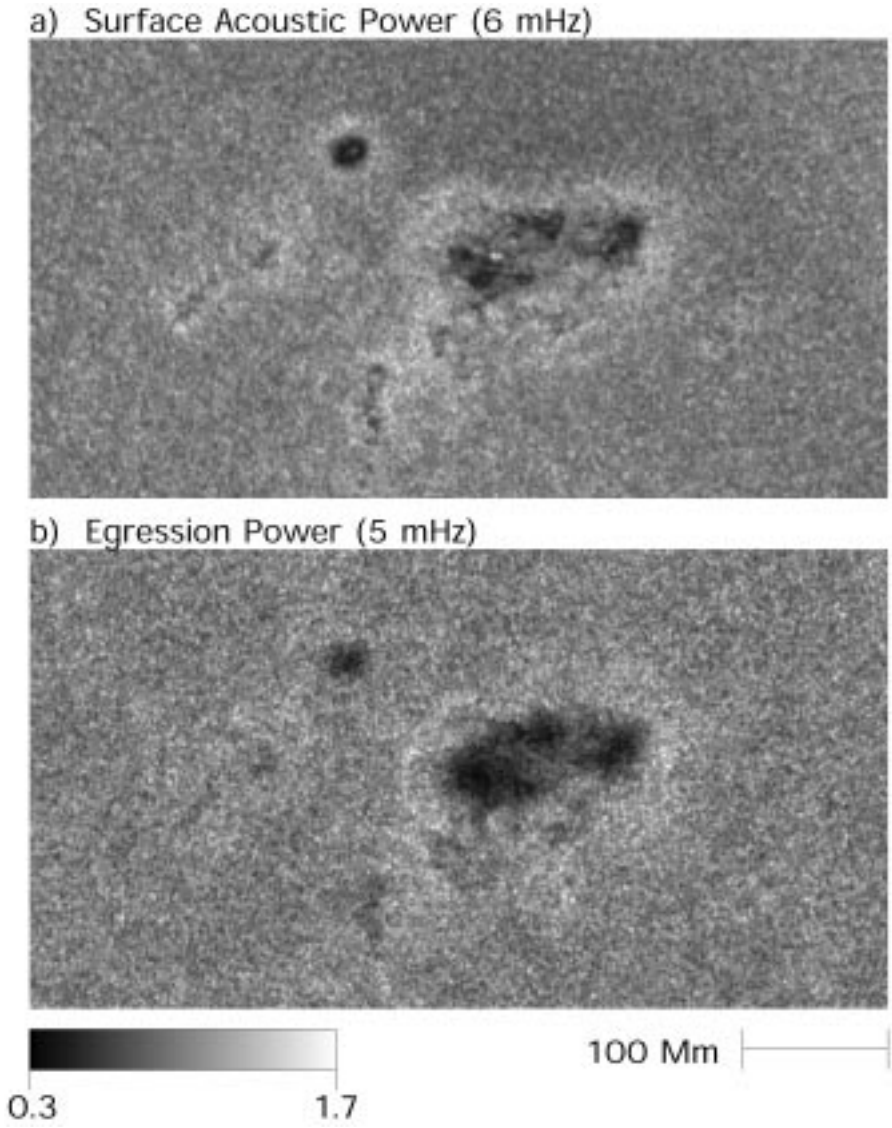

Figure 4. An acoustic power map (a) of NOAA AR 8179 is compared with the egression-power map (b) that appears in Figures 1(a) and 1(c). The isolated, monopolar sunspot to the north-east (upper left) of NOAA AR 8179 has a distinct acoustic power halo, but not a conspicuous acoustic glory. Large, multipolar active regions generally have strong acoustic glories. The annotation of the greyscale at lower left applies to the egression-power map only, which is normalized to unity in the quiet Sun. The same greyscale spans the range 0.0−2.0 in surface acoustic power (a), also normalized to unity in the quiet Sun.

ing is suggestive of the acoustic glories. With careful ground-based observations co-spatial with high-resolution MDI observations, it should be possible to clarify this relationship. The high-resolution MDI observations may allow us to correlate directly local egression-power profiles with such phenomena as intergranular-lane collapses.

At this point, it is still wise to keep in mind the possibility that the sustained emission that emanates from acoustic glories involves a substantially different mechanism than that which operates in the quiet Sun. Recent work by Braun and Lindsey (2000) using phase-sensitive seismic holography has shown that the subphotospheres of large, multipolar active regions, including the outlying regions that encompass the acoustic glory and acoustic moat, significantly reflect upcoming seismic waves throughout the 4.5–6.5 mHz spectrum. This is in sharp contrast to the quiet photosphere, which reflects 5-mHz oscillations poorly and 6-mHz insignificantly. If acoustic glories contain elements that are particularly efficient reflectors of incoming seismic radiation while continuing to produce turbulent emission of their own, then the enhanced egression would be readily explained, even perhaps while the saturation of the distribution in egression power of acoustic glories at high seismic powers remains a puzzle.

The saturation phenomenon seems to be statistically significant and is most interesting. Given the exponential distributions of egression and ingression power from the quiet Sun, it is difficult to conceive of a contrivance whereby the saturation of seismic emission from acoustic glories would be the result of an instrumental artifact. Since any mechanism that produces seismic waves is eventually constrained by limits in the energy source that drives the wave emission, the hydromechanics of wave production must become significantly non-linear at some point in such a way that could indeed be manifested by saturation. That significant saturation should appear at this level may offer us useful insight into the physical mechanism of seismic emission from the solar subphotosphere.

The study presented here, and its recent predecessor, Donea, Braun, and Lindsey (1999), have opened an important aspect to the general diagnostic of helioseismic holography that is quite new in practical application. This is the utility of deriving the temporal character of seismic emission to a discrimination entirely commensurate with the diffraction-limited spatial resolution that solar seismic imaging has given us since the advent of SOHO-MDI. This new avenue of seismic holography clearly promises a practical and powerful tool for the purpose of understanding the hydromechanics of seismic emission from the near solar interior.

Acknowledgements

We greatly appreciate the support we have gotten from the SOHO SOI-MDI team and the fine quality of the data which they have given us. We especially appreciate the conscientious support of Dr P. Scherrer, head of the SOHO-MDI project. SOHO

is a project of international cooperation between ESA and NASA. D.C.B., a visitor at the Joint Institute for Laboratory Astrophysics, is grateful to Ellen Zweibel and the staff of JILA for their hospitality and support. This research is supported by NSF Grant AST 9528249 and NASA Grants NAGW-97029 and NAG5-7236 through SPRC, and by the SOI-MDI NASA Investigation through JILA.

References

Braun, D. C. and Lindsey, C.: 1999, *Astrophys. J.* **513**, L79.
Braun, D. C. and Lindsey, C.: 2000, *Solar Phys.* **192**, 307 (this issue).
Braun, D. C., Lindsey, C., Fan, Y., and Jefferies, S. M.: 1992, *Astrophys. J.* **392**, 739.
Braun, D. C., Lindsey, C., Fan, Y., and Fagan, M.: 1998, *Astrophys. J.* **502**, 968.
Brown, T. M.: 1991, *Astrophys. J.* **371**, 396.
Brown, T. M., Bogdan, T. J., Lites, B. W., and Thomas, J. H.: 1992, *Astrophys. J.* **394**, L65.
Deubner, F.-L., Fleck, B., Schmitz, F., and Straus, Th.: 1992, *Astron. Astrophys.* **266**, 560.
Donea, A.-C., Braun, D. C., and Lindsey, C.: 1999, *Astrophys. J.* **513**, L143.
Goldreich, P. and Kumar, P.: 1988, *Astrophys. J.* **326** 462.
Goode, P. R., Strous, L. H., Rimmele, T. R., and Stebbins, R. T.: 1998, *Astrophys. J.* **495**, L27.
Hindman, B. W. and Brown, T. M.: 1998, *Astrophys. J.* **504**, 1029.
Kosovichev, A. G. and Zharkova, V. V.: 1998, *Nature*, **393**, 317.
Lindsey, C. and Braun, D. C.: 1990, *Solar Phys.* **126**, 101.
Lindsey, C. and Braun, D. C.: 1997, *Astrophys. J.* **485**, 895.
Lindsey, C. and Braun, D. C.: 1998a, *Astrophys. J.* **499**, L99.
Lindsey, C. and Braun, D. C.: 1998b, *Astrophys. J.* **509**, L129.
Lindsey, C. and Braun, D. C.: 1999, *Astrophys. J.* **510**, 494.
Lindsey, C. and Braun, D. C.: 2000, *Solar Phys.* **192**, 261 (this issue).
Lindsey, C., Braun, D. C., Jefferies, S. M., Woodard, M. F., Fan, Y., Gu, Y., and Redfield, S.: 1996, *Astrophys. J.* **470**, 636.
Scherrer, P. H. *et al.*: 1995, *Solar Phys.* **162**, 129.
Toner, C. and LaBonte, B. J. 1993, *Astrophys. J.* **415**, 847.